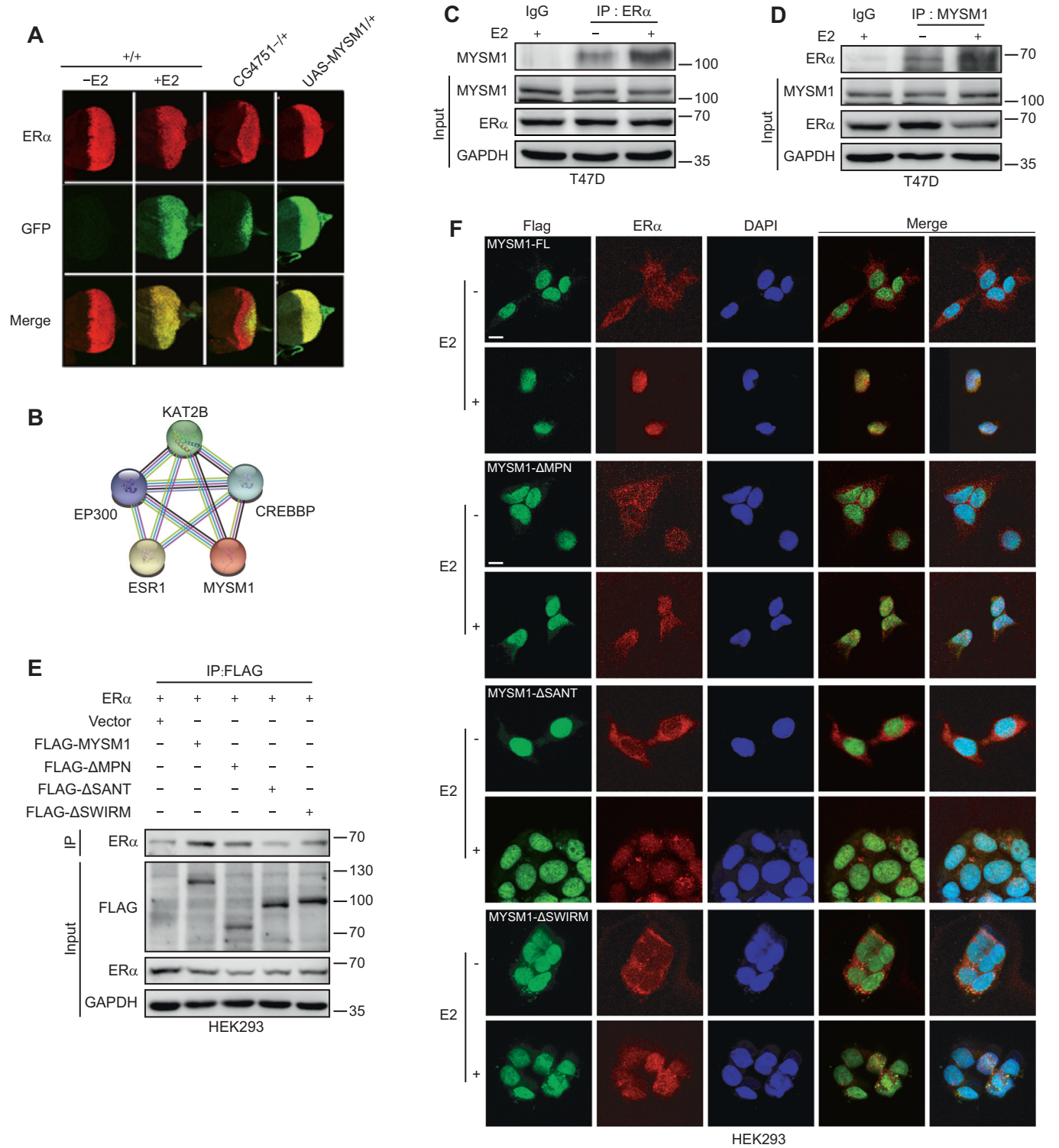
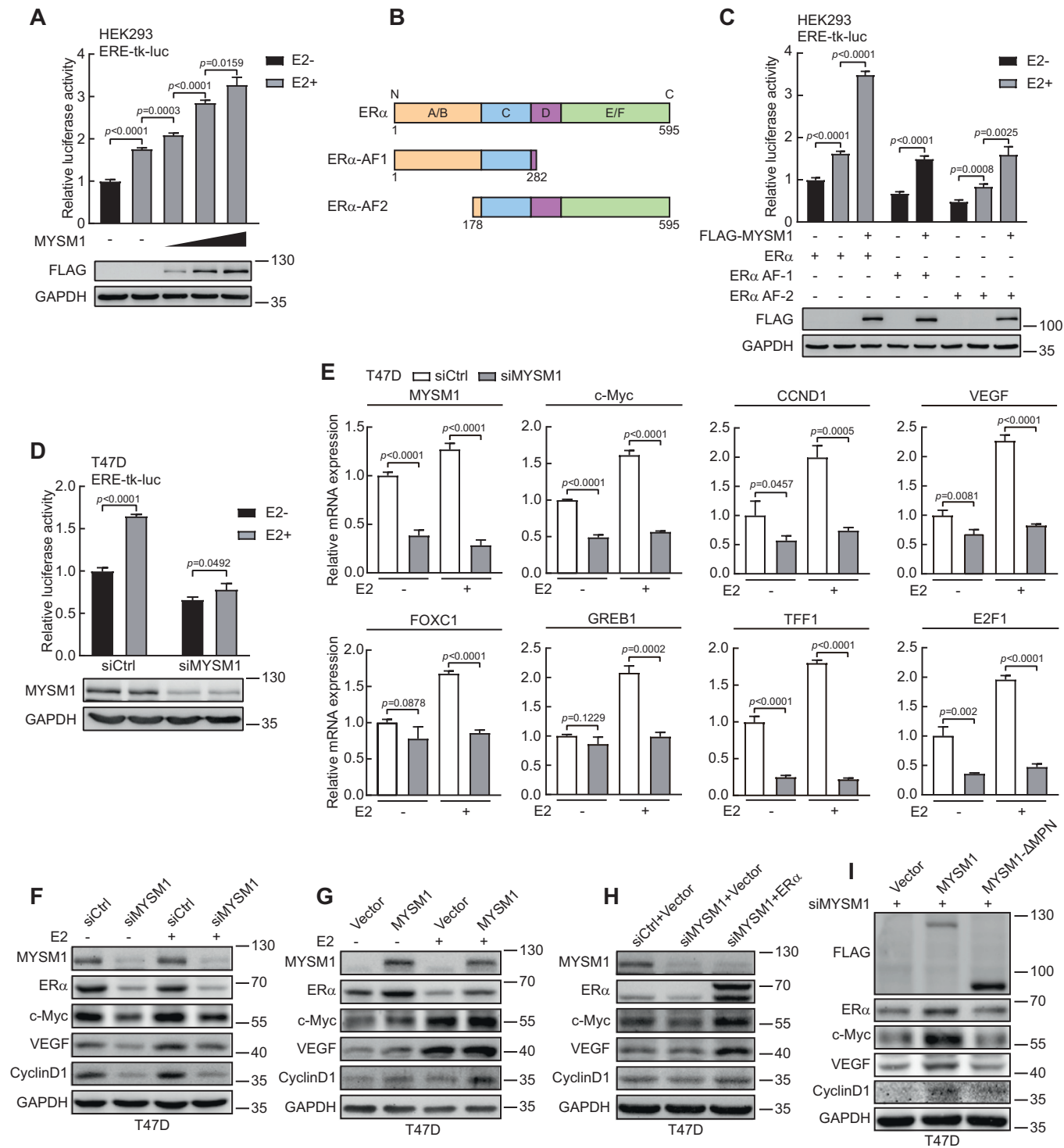


## Expanded View Figures

**Figure EV1. MYSM1 interacts with ER $\alpha$  in breast cancer cells.**

(A) Evaluation of GFP and ER $\alpha$  level in F1 progeny flies with CG4751 loss of function (lane 3) or MYSM1 gain of function (lane 4) mutants. The lower panels represent merge images. (B) The MYSM1-related protein-protein interaction (PPI) networks generated by the STRING online database. (C, D) Co-immunoprecipitation conducted in T47D cells to detect the association between endogenous MYSM1 and ER $\alpha$  in response to E2 treatment. (E) HEK293 cells complemented with ER $\alpha$  or the deletion mutants of MYSM1 were lysed. Complexes precipitated by anti-FLAG were purified and immunoblotted with indicated antibodies. (F) Immunofluorescent staining of MYSM1 (anti-FLAG, green) and ER $\alpha$  (anti-ER $\alpha$ , red) in HEK293 cells overexpressing MYSM1 truncated mutants and ER $\alpha$  in the presence of E2. Nuclei were stained with DAPI (blue). Scale bars, 10  $\mu$ m. Data information: (C-F):  $n = 3$  independent experiments performed in duplicate.





**◀ Figure EV2. MYSM1 enhances ER $\alpha$ -mediated gene transcription in mammalian cells.**

(A) MYSM1 stimulates ER $\alpha$ -mediated gene transcription in a dose-dependent manner. HEK293 cells were transfected with gradually increased amount of ectopic MYSM1 (0.05  $\mu$ g, 0.1  $\mu$ g, or 0.2  $\mu$ g respectively). MYSM1 expression was examined with anti-FLAG by western blot. (B) Schematic representation of ER $\alpha$ , ER $\alpha$ -AF1, and ER $\alpha$ -AF2 plasmids used in luciferase reporter assays. (C) Relative luciferase activities in HEK293 cells transfected with ER $\alpha$  full length or truncated mutants harboring ER $\alpha$  AF-1 or ER $\alpha$  AF-2 together with MYSM1 expression plasmid in the presence or absence of E2 (100 nM). The expression of MYSM1 was detected by western blot. (D) Effect of MYSM1 knockdown on ER $\alpha$ -induced transactivation. The relative luciferase values in T47D cells were examined after transient transfection of siCtrl or siMYSM1 followed by ER $\alpha$  expression plasmid. (E) mRNA levels of several ER $\alpha$  target genes in T47D cells with MYSM1-depleted. (F, G) Immunoblot of ER $\alpha$  target gene expression using the indicated antibodies in MYSM1-depleted T47D cells (F) and MYSM1-overexpressed T47D cells (G) with or without E2 (100 nM) treatment for 16-18 h. (H) The loss of ER $\alpha$  and its target genes in MYSM1-depleted T47D cells can be rescued by ectopic ER $\alpha$  expression. T47D cells were transfected with siCtrl or siMYSM1 followed by PcDNA3.1/ER $\alpha$  expression plasmid. (I) Western blot detecting the protein levels of ER $\alpha$  and its target genes in MYSM1-depleted T47D cells transfected with PcDNA3.1/MYSM1/MYSM1- $\Delta$ MPN expression plasmids. Data information: \* $P < 0.05$ , \*\* $P < 0.01$ , \*\*\* $P < 0.001$  (mean  $\pm$  SD; Student's  $t$  test;  $n = 3$  independent experiments).

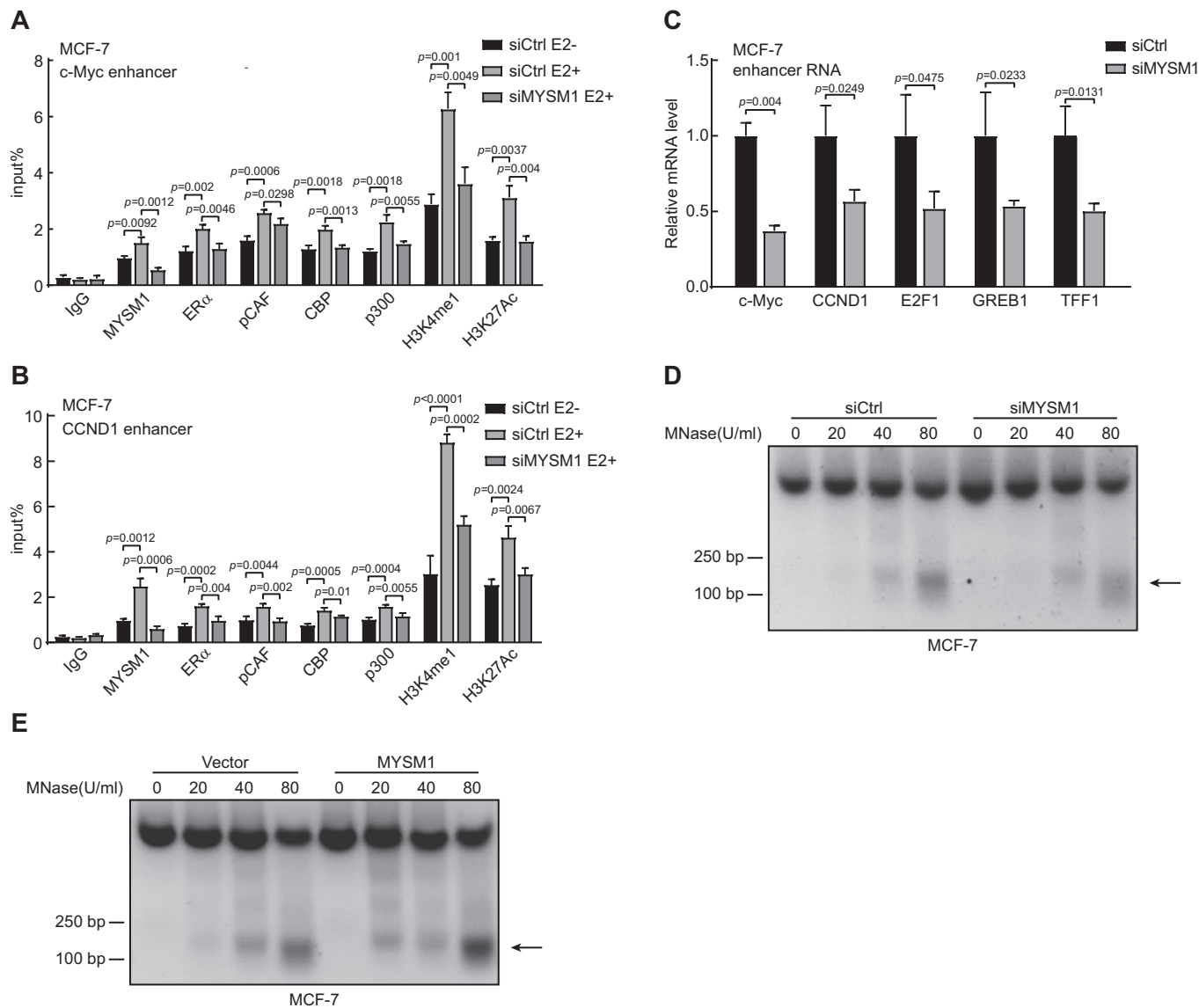
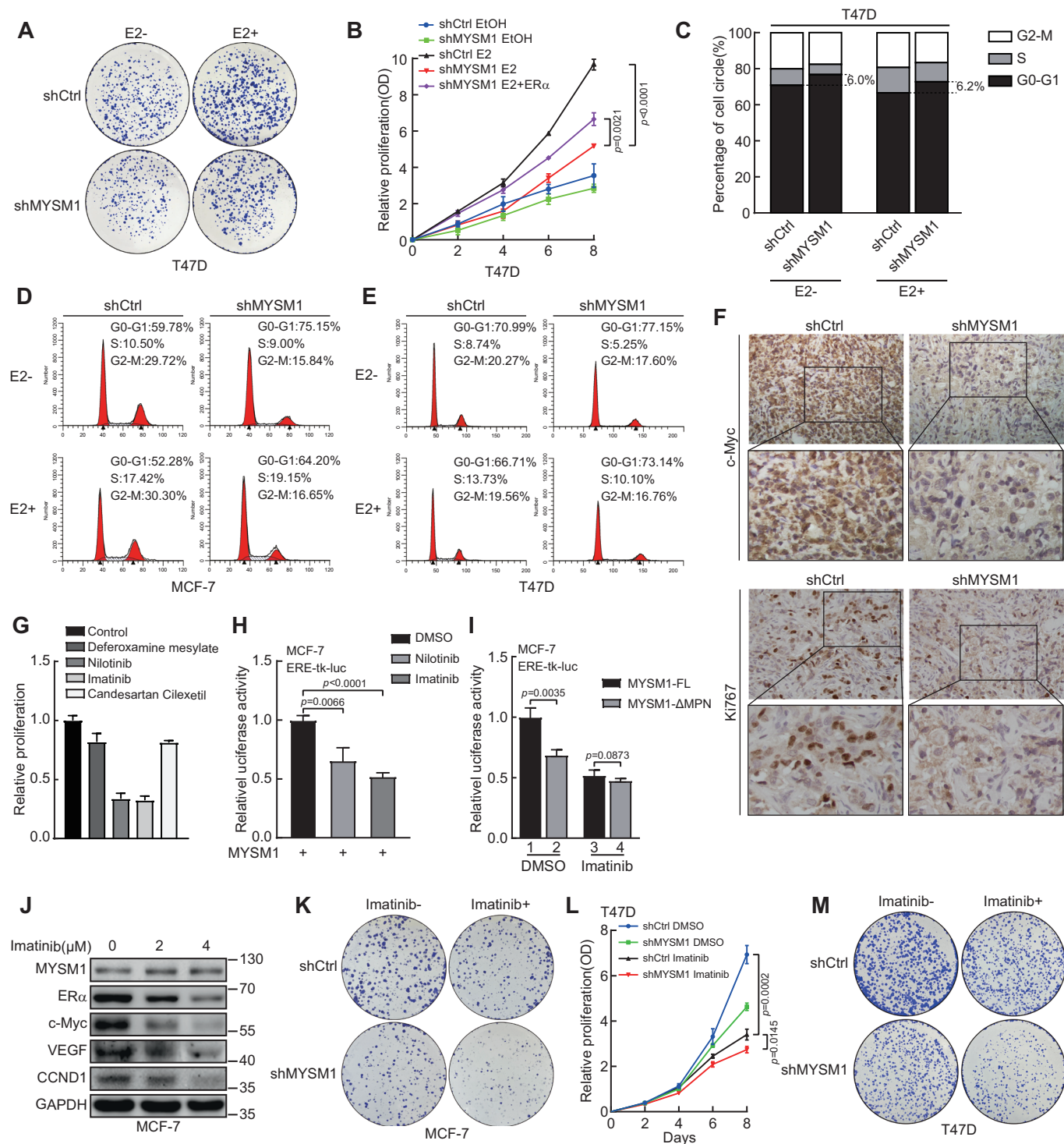


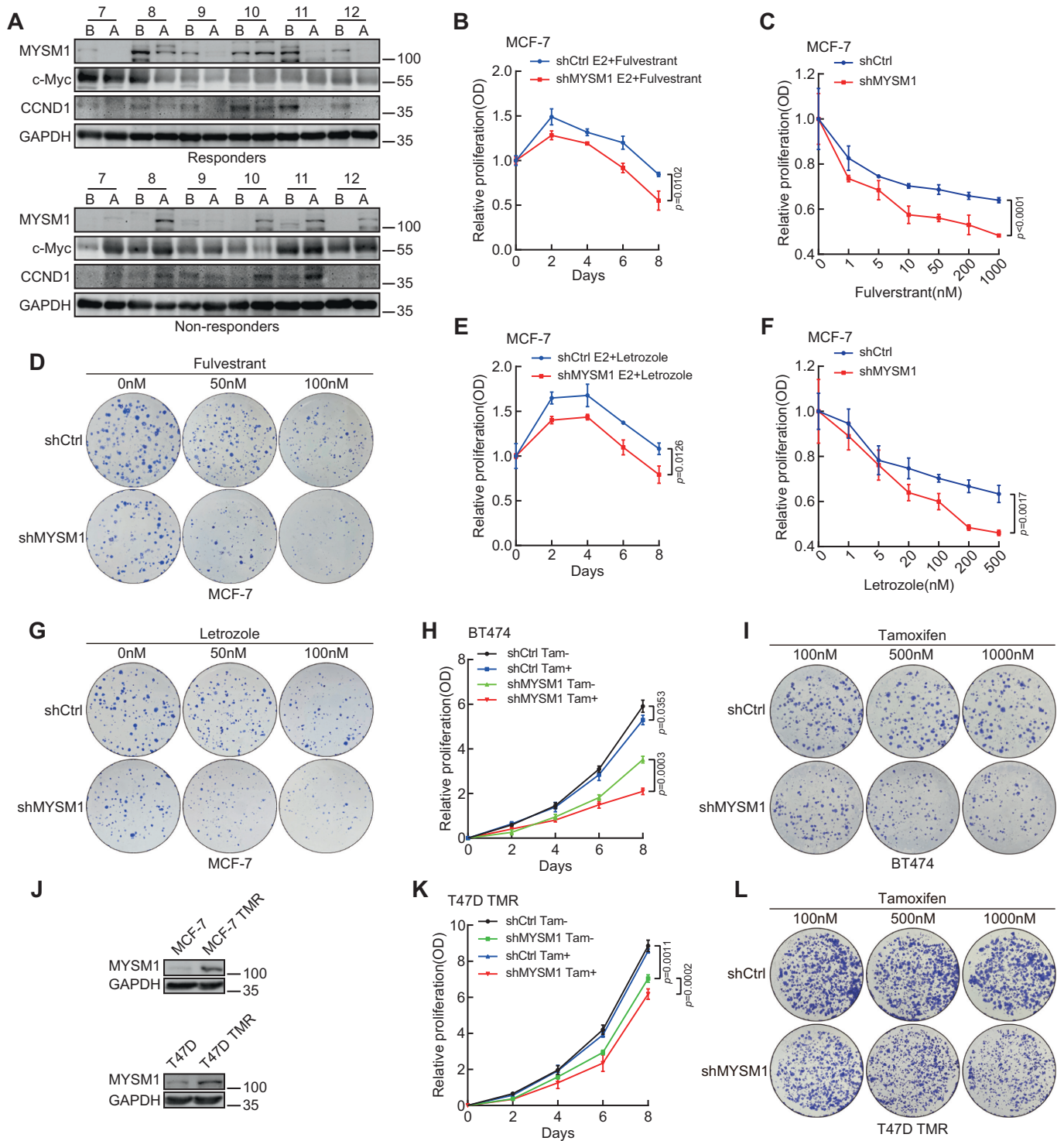
**Figure EV3. MYSM1 enhances the occupation of ER $\alpha$  and HAT complex on E2-regulated enhancers in MCF-7 cells.**

(A, B) ChIP assays via designated antibodies demonstrating the recruitment of MYSM1, ER $\alpha$ , pCAF, CBP, p300 and the histone modification levels H3K4me1 and H3K27ac at the ER $\alpha$  binding site on *c-Myc* (A) or *CCND1* (B) enhancer in MCF-7 cells upon MYSM1 depletion. (C) qPCR analysis demonstrating the eRNA expression of estrogen-induced genes in MCF-7 cells transfected with siCtrl or siMYSM1 in the presence of E2. (D, E) MNase experiments examining chromatin accessibility after digestion with 0, 20, 40, or 80 U MNase in MYSM1-depletion (D) or MYSM1-overexpression (E) MCF-7 cells. Data information: (A-C):  $n = 3$  independent experiments. \* $P < 0.05$ , \*\* $P < 0.01$ , \*\*\* $P < 0.001$ , N.S. means no significance (mean  $\pm$  SD; Student's  $t$  test).



**◀ Figure EV4. MYSM1 depletion or the small molecule Imatinib docked to MYSM1 suppresses breast cancer cell growth through MYSM1-ER $\alpha$  axis.**

(A) Influence of MYSM1 deficiency on T47D cells as illustrated by colony formation. (B) Relative proliferation rates of T47D cells carrying shCtrl or shMYSM1 with or without E2 (100 nM) by MTS assay. (C-E) Flow cytometric analysis of the cell cycle for MCF-7 (D) and T47D (E) with MYSM1 depletion. All figures about flow cytometry represented the results of three independent experiments. The proportion of the T47D cell population in different phases are listed in (C). (F) c-Myc and Ki67 expression by IHC analysis in xenograft tumors derived from MCF-7 (shCtrl) group and MCF-7 (shMYSM1) group. (G) Histograms showing the effects of Deferoxamine mesylate (2  $\mu$ M), Nilotinib (2  $\mu$ M), Imatinib (2  $\mu$ M), or Candesartan Cilexetil (2  $\mu$ M) on MCF-7 cell proliferation. The results are expressed relative to the control (2  $\mu$ M DMSO treated). (H) The effect of Nilotinib (2  $\mu$ M) or Imatinib (2  $\mu$ M) on luciferase activity in MCF-7 cells transfected with ER $\alpha$ -related dual-luciferase reporter system and MYSM1 expression plasmid. (I) The effect of Imatinib (2  $\mu$ M) on luciferase activity in MCF-7 cells transfected with ER $\alpha$ -related dual-luciferase reporter system, MYSM1-FL or MYSM1- $\Delta$ MPN expression plasmid. (J) Western blot showing the expression of the indicated proteins in MCF-7 cells treated with different concentrations of Imatinib (0  $\mu$ M, 2  $\mu$ M, or 4  $\mu$ M respectively). (K) Colony formation assay showing the effect of Imatinib treatment (1  $\mu$ M) on shCtrl or shMYSM1 stably expressed MCF-7 cells. (L) Growth curve showing the effect of shMYSM1, Imatinib, or their combination (1  $\mu$ M) on T47D cell proliferation. Total cell viability was assessed every other day by MTS assay. (M) Colony formation assay showing the effect of Imatinib treatment (1  $\mu$ M) on shCtrl or shMYSM1 stably expressed T47D cells. Data information: \*\* $P < 0.01$ , \*\*\* $P < 0.001$  (mean  $\pm$  SD; Student's  $t$  test;  $n = 3$  independent experiments).





**◀ Figure EV5. MYSM1 depletion subjects ER $\alpha$ -positive breast cancer cells to endocrine treatment.**

(A) MYSM1 and CCND1 protein expression in the “Responders” and “Non-responders” samples before and after AI treatment were examined by western blot. “B” represents cases before AI treatment, “A” represents cases after AI treatment ( $n = 6$ ). (B, E) Growth curve showing the effect of MYSM1 knockdown on MCF-7 cell proliferation with Fulvestrant (200 nM) (B) or Letrozole (100 nM) (E) treatment. Total cell viability was assessed every other day by MTS assay. (C, F) A cellular viability detection in MYSM1-deletion MCF-7 cells that incubated in various concentrations of Fulvestrant (C) or Letrozole (F) for 7 days. (D, G) MCF-7 cells with/without MYSM1 knockdown were subjected to colony formation assay under diverse doses of Fulvestrant (D) or Letrozole (G). Clones were stained with R250 and photographed 2 weeks later. (H, K) The line chart renders the relative proliferation of the shMYSM1 group compared to the shCtrl group in BT474 (H) or T47D TMR (K) cells in the stimulation of Tamoxifen (1  $\mu$ M) or not. (I, L) The panels show colony-formation assay conducted in BT474 (I) or T47D TMR (L) cells infected with lentivirus expressing shCtrl/shMYSM1. Cells in each panel were treated with different doses of Tamoxifen for 15 days before fixation and R250 staining. (J) Western blot assay detecting MYSM1 protein expression in MCF-7, T47D, and their corresponding Tamoxifen-resistant (TMR) cells. Data information: \* $P < 0.05$ , \*\* $P < 0.01$ , \*\*\* $P < 0.001$  (mean  $\pm$  SD; Student’s  $t$  test;  $n = 3$  independent experiments).